Developmental dynamics of the impact of constitutive mTORC1 hyperactivity and environmental enrichment on structural synaptic plasticity and behaviour in a rat model of autism spectrum disorder

Authors: Simon Granak[1,2], Klara Tuckova[1,3], Viera Kutna[1], Iveta Vojtechova[1,4], Laura Bajkova[2], Tomas Petrasek[1,4*†] and Saak V. Ovsepian[5*†]

Affiliations: (1) National Institute of Mental Health, Topolova 748, 25067 Klecany, Czech Republic; (2) Third Faculty of Medicine, Charles University, Ruska 87, 10000 Prague 10, Czech Republic; (3) Faculty of Science, Charles University, Albertov 6, 12800 Prague 2, Czech Republic; (4) Laboratory of Neurophysiology of Memory, Institute of Physiology of the Czech Academy of Sciences, Videnska 1083, 14220 Prague 4, Czech Republic; (5) Faculty of Science and Engineering, University of Greenwich London, Chatham Maritime, Kent, ME4 4TB, United Kingdom.

***Correspondence:** Tomas Petrasek, National Institute of Mental Health, Topolova 748, 25067 Klecany, Czech Republic, Tomas.Petrasek@nudz.cz

Saak V. Ovsepian, Faculty of Science and Engineering, University of Greenwich London, Chatham Maritime, Kent, ME4 4TB, United Kingdom, s.v.ovsepian@gre.ac.uk

†Shared last authorship (equal contributions)

Author contributions: S.G., V.K., T.P. and S.V.O. designed the study; S.G., K.T., V.K., I.V., T.P. and L.B. carried out the experiments and analysed the data; S.G., T.P., I.V. and S.V.O. wrote and revised the manuscript; S.G. and S.V.O. prepared the illustrative materials; V.K., T.P. and S.V.O. supervised the project.

Acknowledgements

This study was supported by the Ministry of Health Czech Republic – IFB 2022 („National Institute of Mental Health – NIMH, IN: 00023752“). S.V.O. acknowledges the Innovation Fund Award from the University of Greenwich.

Conflict of interest: The authors of this study report no potential conflict of interest.

Abstract

Autism spectrum disorder (ASD) is a neurodevelopmental condition causing a range of social and communication impairments. Although the role of multiple genes and environmental factors has been reported, the impact of the interplay between genes and environment on the onset and progression of the disease remains elusive. We housed wild-type (*Tsc2+/+*) and tuberous sclerosis 2 deficient (*Tsc2+/-)* Eker rats (ASD model) in individually ventilated cages or enriched conditions and conducted a series of behavioural tests followed by the histochemical analysis of dendritic spines and plasticity in three age groups (days 45, 90, and 365). The elevated plus-maze test revealed a reduction of anxiety by enrichment, while the mobility of young and adult Eker rats in the open field was lower compared to wild-type. In the social interaction test, an enriched environment reduced social contact in the youngest group and increased anogenital exploration in 90- and 365-day-old rats. Self-grooming was increased by environmental enrichment in young and adult rats and decreased in aged Eker rats. Dendritic spine counts revealed an increased spine density in the cingulate gyrus in adult Ekers irrespective of housing conditions, whereas spine density in hippocampal pyramidal neurons was comparable across all genotypes and groups. Morphometric analysis of dendritic spines revealed age-related changes in spine morphology and density which were responsive to animal genotype and environment. Taken together, our findings suggest that under TSC2 haploinsufficiency and mTORC1 hyperactivity, the expression of behavioural signs and neuroplasticity in Eker rats can be differentially influenced by the developmental stage and environment.

Keywords: animal models of autism; tuberous sclerosis complex, dendritic spine; cingulate gyrus; open field test; enriched environment; Eker rats

Lay Summary

Autism spectrum disorder (ASD) is a multifactorial neurodevelopmetnal disease influenced by an array of genetic and environmental factors. It is not clear how their interplay can influence the onset, progression, and severity of neurobehavioral phenotypes. This study shows the in ASD rats, the impact of environment on cognition, social behaviour and neuroplasticity readouts differ significantly from wild type controls, and depends on their developmental stage.

Introduction

The discrete molecular, histopathological, and neurobehavioral phenotypes of the loss-of-function mutations in the *Tsc2* (tuberous sclerosis complex 2) gene make Eker rats a useful model for studies of TSC, a multisystemic disease featuring benign tumours and lesions in various organs, and a variety of neuropsychiatric symptoms (Henske *et al.*, 2016; Kutna *et al.*, 2021). The main cause of cellular and molecular pathology in both rats and humans is the deficiency of TSC2 protein (known also as tuberin), which leads to hyperactivity of mTORC1 (mammalian target of rapamycin complex 1), an important kinase that controls protein synthesis, cell growth and proliferation, cell cycle, and metabolism (Crino, 2016). It is hardly surprising, therefore, that since the first report on the rat model by R. Eker (Eker, 1954), it has been used mainly for research focused on the mechanisms underlying the development of neoplastic lesions, known as hamartomas (Mizuguchi *et al.*, 2000; Schwartzkroin *et al.*, 2004; Wenzel *et al.*, 2004; Kutna *et al.*, 2020). However, the mTOR pathway is also involved in the regulation of a range of processes implicated in neurodevelopment, synaptic plasticity, and pruning (Hoeffer & Klann, 2010; Ma *et al.*, 2010; Tang *et al.*, 2014). There is ample evidence suggesting that in Eker rat, the impact of spontaneous *Tsc2* loss-of-function extends beyond abnormal tissue growth and proliferation and can affect a variety of functional and regenerative mechanisms in neurons, which can contribute to the important neurobiological process, causing a spectrum of cognitive and behavioural impairments (Waltereit *et al.*, 2011; Crino, 2016; Kutna *et al.*, 2021).

Like in humans, brain malformations of *Tsc2* loss-of-function rats occur in 30-65% of cases and have age-dependent onset (Yeung *et al.*, 1997; Wenzel *et al.*, 2004; Yeung, 2004; Kutna *et al.*, 2020). As the homozygous *Tsc2* loss-of-function (*Tsc2-/-*) variant is lethal (Rennebeck *et al.*, 1998), all Eker rats are heterozygotes, carrying one non-functional allele. In rats, like in human *TSC2+/-* cases, haploinsufficiency of the *Tsc2* gene is associated with

an array of neuropsychiatric signs (Kenerson *et al.*, 2005; Stafstrom, 2005; 2006; Waltereit *et al.*, 2011; Schneider *et al.*, 2017), including social and communication impairments. Autism spectrum disorder (ASD) has been recognized in up to 60 % of humans affected by *TSC2* deficiency, accounting for about 1-4% of the total ASD incidence (Gadad *et al.*, 2013; Curatolo *et al.*, 2018; Specchio *et al.*, 2020). Waltereit and co-workers were the first to study social behaviour in Eker rats, showing that the neurobehavioral phenotype with the deficit in social interactions in adult animals can be influenced by the history of drug-induced seizures during early development (Waltereit *et al.*, 2011). The same group has shown recently that the social deficit, but not seizure-induced impairments in the *Tsc2+/-* Eker rats could be ameliorated by selective inhibition of mTORC1 activity (Petrasek *et al.*, 2021). Evidence from behavioural studies in other models with TSC2 deficiency has demonstrated that autism-like phenotype with characteristic stereotypic behaviour can be achieved by targeted depletion of TSC2 protein in cerebellar Purkinje cells at a later developmental stage (Fu & Ess, 2013; Kutna *et al.*, 2021). Remarkably, autism-like behavioural phenotype could be also induced by targeted silencing of the *Tsc1* gene in Purkinje cells (Tsai *et al.*, 2012; Tsai *et al.*, 2018). Detailed analysis of the impact of *Tsc2* haploinsufficiency on the morphology and cellular organization of the rat cerebellum in different age groups (Kutna *et al.*, 2022) has shown subtle developmental impairments with demyelination of the central track and loss of Purkinje neurons.

As a neurodevelopmental disorder, ASD is characterized by abnormal connectivity in the brain, owing to abnormal synapse formation and functional plasticity (Penzes *et al.*, 2011; Penzes *et al.*, 2013; Joensuu *et al.*, 2018; Erli *et al.*, 2020). Although the causative role of genetic and environmental factors in ASD is well recognized (Chaste & Leboyer, 2012; Talkowski *et al.*, 2014; Bai *et al.*, 2019; Cheroni *et al.*, 2020; Tseng *et al.*, 2021), the effect of their interaction on the onset and progression of the disease remains elusive. It is also unclear

how the interplay between the genes and environment in ASD changes with age, and how these processes relate to functional and structural remodelling and plasticity in the brain. Despite the consensus that mTORC1 hyperactivity plays a prime role in neurobiological and behavioural impairments associated with TSC2 deficiency (Crino, 2016; Kutna *et al.*, 2021), a recent report in neuronal cultures with silencing of the *tsc2* gene showed significant changes in spine morphology, which were resistant to mTORC1 inhibitors (Yasuda *et al.*, 2014). Importantly, the pharmacological block of mTORC1 also failed to counter the effects of *Tsc2* haploinsufficiency (Yasuda *et al.*, 2014), inferring a functional redundancy of this key kinase in regulating synaptic plasticity. Given that the preclinical reports of autism-like symptoms in *Tsc2* deficient models have been limited to a single point or a single age-group analysis (Waltereit *et al.*, 2011; Tsai *et al.*, 2012; Gadad *et al.*, 2013; Reith *et al.*, 2013; Schneider *et al.*, 2017; Kutna *et al.*, 2021; Petrasek *et al.*, 2021), it is unclear how various developmental stages and environmental changes can influence the impact of *Tsc2* deficiency on the neuroplasticity mechanisms and behavioural characteristics.

In this study, we carried out a series of behavioural tests in three age groups of *Tsc2*+/+ (wild-type, WT) and tuberous sclerosis 2 deficient (*Tsc2*+/-) Eker rat model maintained in individually ventilated cages or under environmental enrichment, followed by the histochemical analysis of dendritic spine density and structure, to gain insights into the effects of the development and environment on the neurobehavioral phenotypes and synaptic plasticity.

Materials and Methods

Experimental animals

In total, 69 male rats (Long–Evans Tsc2+/+ or WT (n=37) and Tsc2+/- or Eker (n=32)) from 8 litters were used in the current study. The principal reason for limiting our analysis on

males is that female behaviour is significantly influenced by their estral cycle phase, which is known to affect open field (Miller *et al.*, 2021), plus maze (Marcondes *et al.*, 2001) and social behavior (Frye *et al.*, 2000). It is also justified by the fact that human ASD is much more prevalent in male population, with sex ratio up to 4:1 (Werling & Geschwind, 2013). Animals were divided into four groups based on their genotype and housing conditions (individually ventilated cages, or IVC versus enriched environment), with two genotypes compared at three developmental stages (young, adult, aged), at postnatal days (PND) 45, 90, and 365. The Eker rat line used in the present study was obtained from M. D. Anderson Cancer Center, University of Texas (Rennebeck *et al.*, 1998), via Technische Universität Dresden, Germany. Animals were housed in a Bio-resources facility of the National Institute of Mental Health, Klecany, at constant temperature (+21 ºC), with a 12-h light/12-h dark cycle maintained, food and water provided *ad libitum*. All experimental procedures have been approved by the Institutional Committee for Animal Protection (Project of Experiments No. 46) in line with the Animal Protection Code of the Czech Republic, and the directive of the European Community Council (2010/63/EU). Mating and breeding of the rats were performed in wire lid plastic boxes (44×28×23 cm). After weaning (PND21), the offspring were transferred to the experimental housing. Rats housed without environmental enrichment were kept in pairs in sealed individually ventilated cages (IVC, Tecniplast 40×35×21 cm), which prevented olfactory or acoustic contact with adjacent cages. Opaque partitions and a translucent curtain prevented visual contact with other animals. Rats maintained under enriched conditions (enriched group) lived in groups of five individuals in larger translucent polypropylene boxes (58×37×23 cm) covered with wire lids, equipped with shelters made of plastic tubes, and pieces of wood and tissue paper for gnawing, with olfactory and acoustic contacts allowed between neighbouring cages.

Experiment design

Based on the genotype and housing conditions, rats were divided into: WT housed under (1) IVC (n=17) and (2) enriched conditions (n=21), and Eker housed under (3) IVC (n=17) and (4) enriched (n=16) conditions. Animals were studied at three developmental stages: young (PND45), adult (PND90) and aged (PND365). Overall, we used for the current analysis 26 litters: 10 in PND45, 8 in PND 90 and 8 litters in PND365 age groups. After behavioural tests, rats were transcardially perfused, and their brains were harvested for histochemical and immunofluorescence studies. Figure 1A, B presents the experimental design and summary of the experimental series with the numbers of rats included in the current analysis.

Behavioural tests and animal monitoring

In behavioural experiments, the order of animals was randomized, and the experimenters were blinded to animal genotypes. Rats were always transferred from their housing to the experimental rooms in a clean individual cage and left alone for 10 minutes before being placed in the experimental apparatus. During behavioural tests, all animals were monitored and recorded by an overhead web camera located above the experimental apparatus, with videos evaluated subsequently offline. The BORIS software (Friard & Gamba, 2016) was used for manual scoring of rat behaviour by a blinded human observer while the EthoVision (Noldus) was used for automatic tracking of rat trajectory.

Elevated plus-maze test (EPM)

The apparatus, made from light grey plastic, consisted of four arms (each 10 cm wide, 50 cm long) in a cross shape elevated 70 cm above the floor. Two arms opposite each other were open, the other two were surrounded by 30 cm high walls. The apparatus was illuminated by fluorescent tubes on the ceiling (480 lux in open arms, 85 lux in closed arms). Each animal

was placed into the middle part facing the open arm and recorded for 5 min. We analysed time spent in the open arms (open arm duration), time spent looking down from the maze across the open arm edge (looking down duration), and the number of arm visits as a measure of overall activity. There was no variation between the groups in looking out from the closed arms (risk assessment behaviour), so this parameter was dropped from the analysis.

Open field test (OF)

For the open field test, a square white chipboard arena (70×70 cm), illuminated by fluorescent tubes located on the ceiling (1000 lux), was used. The animal was placed in the middle of the arena, and its behaviour was recorded by a camera for 10 min. In the open field test, we evaluated the locomotor activity of animals, recorded as total travelled distance, and the time spent in the central 50% of the area of the apparatus (centre duration).

Social interaction test (SI)

In this test, two unfamiliar rats of the same experimental group were left to interact in a dimly illuminated (18 lux) neutral environment of the open-field arena. The rats were placed into the apparatus simultaneously, facing the opposite corners, and were recorded for 10 min. Social isolation (10 min) preceded the interaction test. In this test, we evaluated social exploration (sniffing the head and body of the social partner), anogenital sniffing (sniffing to the anogenital region or tail base of the partner), and self-grooming during the first 5 minutes. Other forms of social behaviour, such as aggressive interactions or allogrooming were absent or too rare for statistical evaluation.

Histological experiments and dendritic spine counting

For histology experiments, rats were anaesthetized with an intraperitoneal (i.p.) injection of xylazine (30 mg/kg) and ketamine (200 mg/kg) and transcardially perfused with 0.9% saline followed by 4% paraformaldehyde (150 ml) (Sigma-Aldrich, catalogue # P6418) in 0.1 M phosphate buffer, at pH 7.4. Brains were removed and divided into two hemispheres. The right part was preserved for immunohistochemistry, while the left was used for histological studies using rapid-Golgi staining (Patro *et al.*, 2013). After cryoprotection with 30% sucrose for 48 hrs, the tissue was frozen and serially cut (Leica CM1860 UV) into 100 µm coronal sections. Following sequential incubations in 70% and 100% ethanol (time: each 10 min) and NeoClear (Merck, catalogue # 109843) (time: 10 min), sections were mounted on gelatin-coated slides and coverslipped with mounting medium NeoMount (Merck, catalogue # 109016) for light microscopic analysis (Zeiss Axio Imager Z1 microscope). For morphological analysis and characterization of dendritic spines, we examined the cingulate gyrus and the CA1 area of the dorsal hippocampus, based on an anatomical map of a rat brain (Paxinos & Watson, 2007). Spine counting was carried out manually in an online regime with a Zeiss Axio Imager Z1 microscope using the 63× objective. The counting researcher was blinded to the experimental condition and animal genotype. For analysis of dendritic spines, four pyramidal neurons per rat were selected randomly from defined regions of interest, with spines of the second-order apical dendrites counted over 10-12 µm segments. All protrusions from dendritic shafts were treated and counted as “spines”, with selection criteria for qualifying as spines verified by two independent observers. Due to limitations of the light microscopy method, the estimated numbers of dendritic spines are likely to represent underestimates of the actual spine numbers, due to lapse of dendritic spines beneath or above the dendritic segment (Gonzalez & Kolb, 2003). For sorting dendritic spines into morphological categories such as thin, stubby, and mushroom-like, and their quantification, we have used established morphological criteria (Rochefort & Konnerth, 2012; Granak *et al.*,

2021). Given the limitations of light microscopy for visualizing dendritic spines (Mancuso *et al.*, 2013), we have included in the current analysis only spines that could be unambiguously identified as one of these morphological types.

Immunofluorescence and confocal imaging

The right side of rat brains selected for immunohistochemistry was post-fixed overnight in 4% paraformaldehyde followed by cryoprotection in 30% sucrose. Frozen material was serially sectioned on a cryostat (Leica CM1860 UV) into 50 µm coronal slices, with each fifth collected and stored in a cryoprotective solution (ethylene glycol, glycerol, and disodium phosphate in distilled water) at −20 °C until processed. Free-floating sections were rinsed extensively in 0.1 M PBS. Non-specific immunoreactivity was blocked with 10% normal goat serum (NGS, Merck, catalogue # S26) and 0.3% Triton-X100 for 1 hour at room temperature. This was followed by overnight incubation of brain sections with primary antibodies in 0.1 M PBS containing 0.3% Triton-X 100, at 4 °C. The following primary antibodies were used: anti-glial fibrillary acidic protein (GFAP, rabbit polyclonal, 1:5000, Dako, catalogue # Z033429), anti-Neuronal nuclear antigen (NeuN, mouse monoclonal, 1:1000, Millipore, catalogue # MAB377), anti-phospho-S6 ribosomal protein antibody (pS6, rabbit monoclonal, 1:1000, Cell Signaling, catalogue # 5364). Sections were subsequently rinsed in 0.1 M PBS and incubated with secondary antibodies in 0.1 M PBS containing 0.3% Triton-X 100 for 2 h at room temperature. The following secondary antibodies conjugated with fluorophores were used, according to the chosen primary antibodies (Donkey anti-mouse AF488, catalogue # 715-545-150, and Donkey anti-rabbit AF594, catalogue # 711-585-152, and 1:500, Jackson ImmunoResearch). After exposure to secondary antibodies, sections were rinsed in 0.1 M PBS and coverslipped in ProLong Gold Antifade Reagent with DAPI (Cell Signaling Technology, catalogue # 8961) and viewed with a Leica TCS SP8X confocal

system (10× objective lens, argon laser) (Leica Microsystems Mannheim, Germany). Brain images were acquired using appropriate excitation lines and filters, with data analysis carried out offline using ImageJ 1.47 software (NIH, USA). The intensity of excitation was optimized and maintained consistently throughout all datasets, with image brightness and contrast standardized across image series. Obtained numerical values were tabulated and used for comparative analysis and statistical tests. Figures were produced using Adobe Illustrator (Adobe Systems, San Jose, CA).

Data analysis and statistics

For immunofluorescence signal intensity analysis and neuron counting, low-power fluorescence images were taken from the cingulate gyrus and the dorsal hippocampus of rats. For intensity measurements, images were converted into 8-bit black and white formats. In the cingulate gyrus, signal intensity was estimated on randomly defined regions of interest (ROIs) within layers 2 and 3, while in the hippocampus, ROIs were placed within the CA1 region of the dorsal hippocampus. Neuron counting was carried out manually after splitting GFAP-NeuN double stained fluorescence micrographs of cligulate gyrus area into gray images of neurons and glia, with numbers tabulated and analysed off-line. Mean signal intensity values were pulled from 14-26 optical sections using a dedicated macro of ImageJ. For analysis of fluorescence areas, data were acquired using a dedicated function of ImageJ, as specified elsewhere (Kutna *et al.*, 2022). The mean values of each bar in bar graphs in Figure 5 present the calculated average of 9 individual measurements per rat from three rats per group. The standard error of the mean was calculated as SEM = $\sigma/\sqrt{n}$, where σ is the sample standard deviation, while n is the number of samples. For statistical tests of signal intensity measurements, normal distribution of the data was assumed. For dendritic spine density and spine type analysis, the averaged values were collected from 4 neurons per

animal, with 5-6 animals per experimental group. Two-way analysis of variance (ANOVA) with genotype and environment as between-subject factors was used for statistical evaluation of the data, using IBM SPSS Statistics (data from brain analyses) and GraphPad Prism (behavioural data) software. Each experimental time point was evaluated separately. All results are presented as means ± SEM. The significance threshold was set at p = 0.05, with values below considered statistically significant.

Results

Impact of genotype, age and environment on anxiety and general locomotor activity

Anxiety and general locomotor activity were tested in the elevated plus maze and open field tests in three age groups (Figure 1A-C for experiment design and sample size). In the elevated plus maze, rats housed in enriched environments showed higher number of all arm visits at PND45 ($F(1, 76) = 4.930$; $p = 0.0294$), and PND365 ($F(1, 36) = 6.685$; $p = 0.0139$), suggesting higher levels of activity (Figure 2A). At PND365, there was also a significant interaction between genotype and environment ($F(1, 36) = 9.280$; $p = 0.0043$), showing that the effect of enrichment was more pronounced in Eker rats. Rats from enriched environments spent more time in the open arms of the maze at both PND90 ($F(1, 52) = 7.734$; $p = 0.0075$) and PND365 ($F(1, 36) = 10.89$; $p = 0.0022$) (Figure 2B). Measurement of looking down duration from the open arms showed a significant increase in rats housed in an enriched environment, irrespective of their genotype, at all three timepoints: PND45 ($F(1, 76) = 8.944$; $p = 0.0037$), PND90 ($F(1, 52) = 17.16$; $p = 0.0001$) and PND365 ($F(1, 36) = 12.22$; $p = 0.0013$) (Figure 2C). Overall, these results suggest a lower level of anxiety in rats housed under enriched conditions.

Another commonly used test for locomotor activity and anxiety levels is the open field paradigm, with measurements of the travelled distance and time spent in the centre of

the apparatus (Mechan *et al.*, 2002). Eker rats showed lower locomotor activity at PND45 ($F(1, 48) = 13.34$; $p = 0.0006$) and PND90 ($F(1, 56) = 5.134$; $p = 0.0273$). This behavioural trend was not detected in aged rats, which showed similar mobility (Figure 2D). Unlike travelled distance, the time spent in the centre showed a strong response to the environmental enrichment at PND90 ($F(1, 56) = 25.41$; $p < 0.0001$) and PND365 ($F(1, 36) = 5.099$; $p = 0.0301$), with the rats from enriched environment spending less time in the central area. At PND365, there was also a significant interaction between the animal genotype and environment ($F(1, 36) = 6.945$; $p = 0.0123$), because the effect of environment was apparent only in the WT animals at this developmental stage (Figure 2E). Although we have randomized animals from different litters, we nevertheless conducted a one-way ANOVA analysis with one factor i.e. litter in PND45 rats, which was the largest (10 litters). No effects has been found on travel distance in open field test ($p=0.322$). The results of a two-way ANOVA with factors of genotype and environment, and with factor litter as a covariat, also confirmed the potential absence of litter bias with accuracy of our observations and their interpretations.

Effects of *Tsc2* deficiency on social behaviour are sensitive to age and the environment

Next, we analysed the behaviour of rats during social interaction. Duration of social contact was shorter in young (PND45) rats maintained in enriched conditions ($F(1, 64) = 10.27$; $p = 0.0021$) (Figure 3A). A similar comparison of adult and aged groups in IVC and enriched housing conditions did not reveal any difference. Anogenital sniffing was affected by environment at PND90 ($F(1, 56) = 7.934$; $p = 0.0067$) and PND365 ($F(1, 36) = 15.69$; $p = 0.0003$), with animals housed in enriched cages spending significantly more time exploring their partners (Figure 3B). Aged Eker rats response to environmental enrichment was enhanced in comparison to WT rats (interaction between genotype and environment at P365,

F (1, 36) = 5.444; p = 0.0253). Finally, rats were assessed for self-grooming. This behaviour was sensitive to environment, as it was increased by enrichment at PND45 (F (1, 64) = 11.13; p = 0.0014) and PND90 (F (1, 56) = 7.105; p = 0.0100). Interestingly, at PND365, environmental enrichment showed no effect, but there was a significant effect of genotype (F (1, 36) = 11.82; p = 0.0015) with Eker rats exhibiting less grooming, and interaction between genotype and environment (F (1, 36) = 5.094; p = 0.0302), as the effect of genotype was especially pronounced in rats housed in an enriched environment (Figure 3C). It must be stressed that the difference in self-grooming at P365 could result from normal sample-to-sample variations given the low number of animals, hence this result should be taken with a degree of caution.

The impact of *Tsc2+/-* deficiency on dendritic spines depends on age and environment

Next, we studied if the described age, genotype, and environment-dependent differences reflect underlying differences in synaptic density and dendritic spine morphology. After behavioural tests, rats were perfused and brains were analysed for dendritic spine density and morphology in the cingulate gyrus and hippocampus, two key structures implicated in ASD. Although *Tsc2* deficit is known to cause impairments of spine formation in neurons *in vitro* (Yasuda *et al.*, 2014), it is unclear if these alterations are age-dependent and react to environmental variations. Figure 4A and B show low-power micrographs of Golgi-stained brain slices with typical pyramidal cells included in this analysis (Bregma +2.5 and -3.5) (Paxinos & Watson, 2007). Dendritic spines were counted on the first branches from the main apical shaft (4 branches per animal) on 4 neurons per animal with 5-6 animals in each group, and classified based on their morphology in thin, mushroom, and stubby groups (Rochefort & Konnerth, 2012).

Two-way ANOVA with genotype and environment factors did not show any difference in spine density between age-matched groups in the CA1 (Figure 4C). At PND45, we observed a slight trend of an interaction ($F(1, 16) = 3.105$; $p = 0.097$) between the effect of genotype and environment. At PND365, we observed a stronger trend ($F(1, 16) = 3.882$; $p = 0.066$) toward a higher density of spines in Eker rats. Overall, however, the data showed a gradual age-dependent decline in spine density across all groups in the CA1 of the hippocampus. Similar measurements in the cingulate gyrus showed a significant effect of genotype at PND90, with spine density increased ($F(1, 16) = 64.398$; $p < 0.001$) in the Eker rats (Figure 4D). The density of dendritic spines in WT rats at PND90 was comparable to that at PND45. At PND365, we found a significant effect of enrichment ($F(1, 16) = 4.624$; $p = 0.047$), with Eker rats housed in environmental enrichment showing a lower spine density (Figure 4D).

Analysis of the spine morphology showed that in the hippocampal CA1 region (Figure 4E), the dendritic spines of WT and Eker rats showed considerable variability in young, adult, and aged groups, with mushroom type dominating in young and aged Eker genotype, without visible effects of housing conditions. Interestingly, all four experimental groups, irrespective of the genotype and housing conditions, showed a strong increase in the number of thin spines at PND90 as compared to PND45 followed by a reduction in mushroom spines, with mushroom type rebounding back in the older rats (Figure 4E). Similar measurements in the cingulate gyrus revealed a general trend of an increase in stubby spines with a reduction in mushroom spines at PND365 in both genotypes. In rats housed in an enriched environment, we observed a considerable age-related increase in the density of thin spines from PND45 to PND90, which was especially pronounced in the Eker genotype (Figure 4F).

Comparison of pS6 and GFAP expression between Eker and control rats housed in different environments

Next, we looked for changes in mTORC1 and glial activity markers in the cingulate gyrus and CA1 region using pS6 and GFAP staining (Figure 5). Ribosomal protein S6 phosphorylation is a key readout of mTORC1 activity with its changes reported in various brain disorders, including ASD and neurodegenerative diseases. Figure 5A, D shows representative micrographs of the prefrontal cortex and hippocampus stained for pS6, GFAP, and NeuN (neuronal marker). The results of fluorescence intensity studies are summarized in Figure 5B-F. In adult PND90 Eker groups, there is a higher level of pS6 in the pyramidal layer of the CA1 region, in agreement with mTORC1 hyperactivity ($F(1, 8) = 6.960$; $p = 0.03$). Results of similar measurements of pS6 in the cingulate gyrus are shown in Figure 5C, with both genotype and environment having significant effects on its levels at PND365. There was a notable increase in the mean intensity of pS6 protein in Eker rats in layer 2 ($F(1, 8) = 20.385$; $p = 0.002$; not shown) and layer 3 neurons ($F(1, 8) = 22.905$; $p = 0.001$; Figure 5C). Importantly, from this analysis, it emerges a strong environmental effect on the expression of pS6 in layer 2 ($F(1, 8) = 5.713$; $p = 0.044$; not shown) and layer 3 ($F(1, 8) = 13.363$; $p = 0.006$), with higher pS6 expression in enriched animals, with a reduction in pS6 in expression evident in the aged groups. Neuronal counting was carried out in cingulate cortex of 12 rats in total, 3 per group, using 3 slices per rat. A two-way ANOVA statistical analysis showed no change in neuronal density: Genotype: $F(1,8) = 1.895$; $p = 0.206$; Enrichment: $F(1,8) = 0.146$; $p = 0.712$; Genotype - Enrichment (interaction): $F(1,8) = 0.006$; $p = 0.941$. We also compared the distribution and intensity of astrocyte marker GFAP (Figure 5D, E, and F). Two-way ANOVA with factors of genotype and environment showed no significant differences in the GFAP intensity in all age groups in the stratum oriens of the CA1 region of the hippocampus or layers 2 and 3 of the cingulate gyrus.

Discussion

Loss-of-function mutations of *TSC2* are amongst the best-characterized genetic aberrations reported in ASD, with *Tsc2* deficit also causing an autism-like neurobehavioral phenotype in animal models (Gadad *et al.*, 2013; Henske *et al.*, 2016; Specchio *et al.*, 2020). It is generally assumed that behavioural abnormalities in ASD humans and model animals share cellular and molecular pathology. Indeed, multiple reports suggest specific histochemical and functional changes in the hippocampus, cerebellum, and cerebral cortex in rat and mouse models, reminiscent of those in human ASD autopsies (Gadad *et al.*, 2013; Kutna *et al.*, 2021; Kutna *et al.*, 2022). These changes have been demonstrated to affect glutamatergic and GABAergic neurons and synapses, cause immune response impairments and disrupt the mTORC1 signalling (Gadad *et al.*, 2013; Won *et al.*, 2013; de la Torre-Ubieta *et al.*, 2016). As a complex multifactorial disease, the onset and outcome of ASD in humans, in addition to genetic determinants, is modulated by environmental effects. The influences of multiple factors have been implicated in heterogeneity in ASD neuropathology and manifestations. Currently, there is a pressing need in determining how the interplay of multiple factors such as genes, environment, and age can influence the onset, progression, and severity of the pathology with neurobehavioral phenotypes.

We analysed the effects of age and environmental enrichment on the anxiety level, locomotor activity and social interactions in Eker (*Tsc2*+/-) rats, followed by histological assessments of dendritic spine density and morphology, and compared the results with similar readouts in WT (*Tsc2*+/+) controls. In the elevated plus-maze test, we found that number of arm visits, looking down duration, and time spent in the open arms in IVC housed adult and specially aged groups were notably lower than those in the enriched groups, suggesting higher anxiety levels in the former. Interestingly, the decrease in anxiety levels by the

environmental enrichment was most pronounced in the older rats. These findings are in support of the overall anxiolytic effects of environmental enrichment reported in animal studies (Sztainberg *et al.*, 2010; Lopes *et al.*, 2019) and agree with the developmental progression of neurobehavioral phenotypes in *Tsc2*+/- animal models (Feliciano, 2020; Kutna *et al.*, 2020; Kutna *et al.*, 2021; Kutna *et al.*, 2022) as well as ASD in humans (Ozonoff *et al.*, 2008; Davidovitch *et al.*, 2013). Of note, in the open field test, the environmental enrichment had the opposite effect in older age groups, reducing the exploration of the central part of the arena (PND90 and PND365), which is usually taken as a sign of elevated anxiety. Also, increased self-grooming in the social interaction test might be interpreted as stress- or anxiety-induced displacement behaviour, as it mostly occurred in short bursts, unlike grooming under non-stressful circumstances (Kalueff & Tuohimaa, 2005b; a). The anxiety level in rats likely depended on the similarity of the experimental apparatus with their housing cages, with rats housed in an enriched environment feeling calmer in the plus-maze with its enclosed compartments and elevated walkways, while the featureless open-field arena was more natural for the rats housed in the IVC cages. Nevertheless, the aged Eker rats showed lower self-grooming, which became more pronounced after exposure of rats to environmental enrichment. It must be emphasized also that the readouts from the elevated plus-maze and open field tests, although taken as measures of anxiety, are not correlated and can reflect different behavioural dimensions (Ramos, 2008; Sudakov *et al.*, 2013). Of note, in the open field test, the young (PND45) and adult (PND90) Eker rats showed lower mobility (measured as the travelled distance) as compared to the age-matched WT controls, with the differences levelling at up at PND365. On the other hand, in the same test, we observed no genotype-dependent differences in centre duration. The causes for decreased locomotion of Eker rats in the open field test and amelioration of this difference in the aged rats are not clear but might be related to an overall

reduction of motor activity reported in human ASD (Peier *et al.*, 2000; Stins & Emck, 2018), as well as to changes in structures controlling locomotor activity and coordination such as the cerebellum and brain stem (Gadad *et al.*, 2013; Kutna *et al.*, 2022).

The social interaction test revealed that environmental enrichment affected social behaviour towards unfamiliar conspecifics, increasing the tendency to explore the anogenital area of the partner in adult and aged rats while decreasing exploration of the head and body in young rats. The effects of the environment on anogenital exploration were more pronounced in the Eker rats. Several previous studies have reported impaired social behaviour of the Eker rats, which was not observed in the present data. Waltereit et al. showed a reduction in social interactions in rats after induction of status epilepticus at a very young age (Waltereit *et al.*, 2011). Petrasek and co-workers recently reported a deficit of anogenital social exploration in Eker rats from the same breeding colony (Petrasek *et al.*, 2021). The discrepancy between the results of the previous study with the current report can perhaps be explained by the fact that the rats in this study (both genotypes) generally were socially less active (compare Figure 2b, c in Petrasek et al., 2021, with Figure 3A, B in the present study), seemingly contributed by differences in housing conditions. Also, the earlier studies used non-IVC cages, with cage type known to influence the rat performance in behavioural tests (Brain & Benton, 1979; Wurbel, 2001; Van de Weerd *et al.*, 2002).

The reliance of exploratory, anxiety, and social behaviours on the limbic system (which include cingulate gyrus and hippocampus) and related circuits (Martin *et al.*, 2010; Winter *et al.*, 2013; Eslinger *et al.*, 2021) prompted our histochemical investigations of changes in dendritic spine density and morphology, which are known to be altered in human ASD (Penzes *et al.*, 2011; Penzes *et al.*, 2013; Joensuu *et al.*, 2018; Erli *et al.*, 2020) and in ASD experimental animal models (Peier *et al.*, 2000; Gadad *et al.*, 2013). Although *in vitro* evidence suggests an important role of TSC2 protein in governing the dendritic spine

morphology and density, in rapamycin-dependent and rapamycin-independent way (Zhou *et al.*, 2006; Yasuda *et al.*, 2014), to the best of our knowledge, the impact of *Tsc2* loss-of-function on dendritic spine morphology *in vivo* has been only studied at a single developmental stage of transgenic mice (Tavazoie *et al.*, 2005; Meikle *et al.*, 2008). The similarity of spine density in the hippocampal CA1 region between the two genotypes of three age groups irrespective of housing conditions suggests that behavioural differences described herein do not rely on structural plasticity mechanisms of this limbic region. Environment and genotype-dependent variations in spine density and morphology in the cingulate gyrus, on the other hand, imply that the behavioural changes tax synaptic plasticity mechanisms of this brain region. Indeed, our morphometric analysis of dendritic spines revealed a higher proportion of spines with stubby morphology and reduced mushroom spines in aged rats of both genotypes. On the other hand, we found an age-related alteration in the density of thin spines, which were more prominent in the Eker genotype. Likewise, the genotype-dependent differences in spine density varied with the age of animals, with overall spine numbers in adult Eker rats significantly exceeding those in age-matched controls. Unfortunately, in the absence of mechanistic data, it is not possible to interpret these differences in the context of described behavioural observations. It is anticipated that with future studies of developmental dynamics in dendritic spines in Eker rats and other animal models of ASD, it would be possible to shed light on neurobiological mechanisms and the functional significance of these changes. Nevertheless, the occurrence of the behavioural and histochemical changes in adult and aged groups (PND90 and PND365) agrees with increased expression of pS6 protein, signifying higher activity of mTORC1 as a potential cause.

In summary, the results of our behavioural study and histochemical analysis show that the expression of neurobehavioral and neuroplasticity signs in rats with *Tsc2* loss-of-function and constitutive mTORC1 hyperactivity are strongly influenced by the age of experimental

animals and housing conditions. Complex interdependence of multiple factors in the expression of neurobehavioral phenotypes in *Tsc2+/-* Eker rats described herein agrees with the multifactorial nature of ASD and calls for in-depth mechanistic studies with identification of underlying processes, with the prospect of their therapeutic modifications.

Figure legends

Figure 1. Experiment design with illustrations of behavioural tests and morphometric analysis. (A) Experiment design. After the weaning at the postnatal day (PND) 21, rats were transferred to either an enriched environment or individually ventilated cages (EE or IVC, respectively) and subjected to behavioural tests followed by histological analysis in three age groups: PND45 (young), PND90 (adulthood) and PND365 (aged). (B) Table showing the number of rats used in various experiments of the current study. (C) Schematized representation of principal experimental paradigms utilized in this study.

Figure 2. The impact of age, genotype, and environment on behavioural outcomes in the elevated plus-maze (A, B, C) and open field (D, E) tests. Summary bar graphs of the number of arm visits (A), time spent in the open arms (B) and duration of looking down from the maze (C). Summary bar graphs of travelled distance (D) and time spent in the centre of the open field apparatus (E). PND45 left bars; PND90 middle bars; PND365 right bars. Asterisks mark where the difference between groups reached statistical significance * $p < 0.05$, ** $p < 0.005$, *** $p < 0.0005$. White bars represent datasets with no significant difference. GEN – genotype, ENV – environment.

Figure 3. The impact of age, genotype, and environment on behavioural outcomes in social interaction test. Summary bar graphs of the duration of active social contact - head or body sniffing (A), anogenital exploration duration (B) and self-grooming duration (C). PND45, left bars; PND90 middle bars; PND365 right bars. Asterisks mark where the difference between groups reached statistical significance * $p < 0.05$, ** $p < 0.005$, *** $p < 0.0005$. White bars represent datasets with no significant difference. GEN – genotype. ENV – environment.

Figure 4. The impact of the age, genotype, and environment on dendritic spine density and morphology. (A, B) Representative low-magnification images of Golgi rapid stained slices: the cingulate gyrus, bregma +2.5 mm; dorsal hippocampus, bregma -3.5. Rectangles mark the anatomical locations where dendritic spines were analysed. D – dorsal, M – medial. Scale bars: 1.0 mm. (A) Representative light microscopic images of pyramidal neurons with apical and basal dendrites in layer II-III of the cingulate gyrus (middle and right) and (B) CA1 region of the hippocampus (middle and right). Scale bars 15 μm. High-magnification images of secondary dendritic branches with dendritic spines from the prefrontal cortex and hippocampus (A, B: right panels). Black arrows point at individual spines. Scale bars 5 μm. Summary bar graphs of the mean spine density in the CA1 region of the hippocampus (C) and cingulate gyrus (CG) (D). Postnatal days: PND45, left bars; PND90 middle bars; PND365 right bars. Asterisks mark statistically significant differences indicated by two-way ANOVA, with a degree of significance * $p < 0.05$, ** $p < 0.005$. White bars represent datasets with no difference. (E, F) Summary stacked bars representing the fraction (number insets) of three main morphological variants of dendritic spines: thin spines, marked in blue; stubby spines in orange, and mushroom spines in grey. The graphs present data from five rats of each experimental group for individual data points ($n = 5$). GEN – genotype, ENV – environment.

Figure 5. The impact of age, genotype, and environment on neuronal and astrocyte markers NeuN and GFAP and mTOR activation marker pS6. (A, D) Representative immunofluorescence images of hippocampal CA1 (left panels) and cingulate gyrus (CG) areas (right panels) in coronal brain slices stained for the neuronal marker NeuN (green), a marker of mTOR activation pS6 (red; A), and an astrocyte marker GFAP (red; D). Narrow

right insets show an enlarged view of stratum oriens (SO) of the CA1 region of the hippocampus (left panels) and layer III of the CG (right panels). CA1 scale bars 75 μm. Cingulate gyrus scale bars 100 μm. (B, C) Summary bar graphs of the mean intensity of pS6 signal in the stratum pyramidale (PYR Layer) of the CA1 region (B) and layer III of the cingulate gyrus (C). (E, F) Summary graphs of the mean intensity of GFAP in the stratum oriens of the CA1 region (E) and layer 3 of the CG (F). Asterisks mark the results of comparison reaching statistical significance, using two-way ANOVA, with a degree of significance * $p < 0.05$, ** $p < 0.005$. White bars represent datasets with no significant difference. Postnatal day (PND) 45, left bars; PND90 middle bars; PND365 right bars. The graphs present data from three rats of each experimental group for each data point (n = 3), with intensity measurements pulled from 9 regions of interest (ROIs) quantified per animal. GEN – genotype, ENV – environment.

References

Bai, D., Yip, B.H.K., Windham, G.C., Sourander, A., Francis, R., Yoffe, R., Glasson, E., Mahjani, B., Suominen, A., Leonard, H., Gissler, M., Buxbaum, J.D., Wong, K., Schendel, D., Kodesh, A., Breshnahan, M., Levine, S.Z., Parner, E.T., Hansen, S.N., Hultman, C., Reichenberg, A. & Sandin, S. (2019) Association of Genetic and Environmental Factors With Autism in a 5-Country Cohort. *JAMA Psychiatry*, **76**, 1035-1043.

Brain, P. & Benton, D. (1979) The interpretation of physiological correlates of differential housing in laboratory rats. *Life Sci*, **24**, 99-115.

Chaste, P. & Leboyer, M. (2012) Autism risk factors: genes, environment, and gene-environment interactions. *Dialogues Clin Neurosci*, **14**, 281-292.

Cheroni, C., Caporale, N. & Testa, G. (2020) Autism spectrum disorder at the crossroad between genes and environment: contributions, convergences, and interactions in ASD developmental pathophysiology. *Mol Autism*, **11**, 69.

Crino, P.B. (2016) The mTOR signalling cascade: paving new roads to cure neurological disease. *Nat Rev Neurol*, **12**, 379-392.

Curatolo, P., Moavero, R., van Scheppingen, J. & Aronica, E. (2018) mTOR dysregulation and tuberous sclerosis-related epilepsy. *Expert Rev Neurother*, **18**, 185-201.

Davidovitch, M., Hemo, B., Manning-Courtney, P. & Fombonne, E. (2013) Prevalence and incidence of autism spectrum disorder in an Israeli population. *J Autism Dev Disord*, **43**, 785-793.

de la Torre-Ubieta, L., Won, H., Stein, J.L. & Geschwind, D.H. (2016) Advancing the understanding of autism disease mechanisms through genetics. *Nat Med*, **22**, 345-361.

Eker, R. (1954) Familial renal adenomas in Wistar rats; a preliminary report. *Acta Pathol Microbiol Scand*, **34**, 554-562.

Erli, F., Palmos, A.B., Raval, P., Mukherjee, J., Sellers, K.J., Gatford, N.J.F., Moss, S.J., Brandon, N.J., Penzes, P. & Srivastava, D.P. (2020) Estradiol reverses excitatory synapse loss in a cellular model of neuropsychiatric disorders. *Transl Psychiatry*, **10**, 16.

Eslinger, P.J., Anders, S., Ballarini, T., Boutros, S., Krach, S., Mayer, A.V., Moll, J., Newton, T.L., Schroeter, M.L., de Oliveira-Souza, R., Raber, J., Sullivan, G.B., Swain, J.E., Lowe, L. & Zahn, R. (2021) The neuroscience of social feelings: mechanisms of adaptive social functioning. *Neurosci Biobehav Rev*, **128**, 592-620.

Feliciano, D.M. (2020) The Neurodevelopmental Pathogenesis of Tuberous Sclerosis Complex (TSC). *Front Neuroanat*, **14**, 39.

Friard, O. & Gamba, M. (2016) BORIS: a free, versatile open-source event-logging software for video/audio coding and live observations. *Methods Ecol. Evol.* , **7**.

Frye, C.A., Petralia, S.M. & Rhodes, M.E. (2000) Estrous cycle and sex differences in performance on anxiety tasks coincide with increases in hippocampal progesterone and 3alpha,5alpha-THP. *Pharmacol Biochem Behav*, **67**, 587-596.

Fu, C. & Ess, K.C. (2013) Conditional and domain-specific inactivation of the Tsc2 gene in neural progenitor cells. *Genesis*, **51**, 284-292.

Gadad, B.S., Hewitson, L., Young, K.A. & German, D.C. (2013) Neuropathology and animal models of autism: genetic and environmental factors. *Autism Res Treat*, **2013**, 731935.

Gonzalez, C.L. & Kolb, B. (2003) A comparison of different models of stroke on behaviour and brain morphology. *Eur J Neurosci*, **18**, 1950-1962.

Granak, S., Hoschl, C. & Ovsepian, S.V. (2021) Dendritic spine remodeling and plasticity under general anesthesia. *Brain Struct Funct*, **226**, 2001-2017.

Henske, E.P., Jozwiak, S., Kingswood, J.C., Sampson, J.R. & Thiele, E.A. (2016) Tuberous sclerosis complex. *Nat Rev Dis Primers*, **2**, 16035.

Hoeffer, C.A. & Klann, E. (2010) mTOR signaling: at the crossroads of plasticity, memory and disease. *Trends Neurosci*, **33**, 67-75.

Joensuu, M., Lanoue, V. & Hotulainen, P. (2018) Dendritic spine actin cytoskeleton in autism spectrum disorder. *Prog Neuropsychopharmacol Biol Psychiatry*, **84**, 362-381.

Kalueff, A.V. & Tuohimaa, P. (2005a) Contrasting grooming phenotypes in three mouse strains markedly different in anxiety and activity (129S1, BALB/c and NMRI). *Behav Brain Res*, **160**, 1-10.

Kalueff, A.V. & Tuohimaa, P. (2005b) The grooming analysis algorithm discriminates between different levels of anxiety in rats: potential utility for neurobehavioural stress research. *J Neurosci Methods*, **143**, 169-177.

Kenerson, H., Dundon, T.A. & Yeung, R.S. (2005) Effects of rapamycin in the Eker rat model of tuberous sclerosis complex. *Pediatr Res*, **57**, 67-75.

Kutna, V., O'Leary, V.B., Hoschl, C. & Ovsepian, S.V. (2022) Cerebellar demyelination and neurodegeneration associated with mTORC1 hyperactivity may contribute to the developmental onset of autism-like neurobehavioral phenotype in a rat model. *Autism Res*, **15**, 791-805.

Kutna, V., O'Leary, V.B., Newman, E., Hoschl, C. & Ovsepian, S.V. (2021) Revisiting Brain Tuberous Sclerosis Complex in Rat and Human: Shared Molecular and Cellular Pathology Leads to Distinct Neurophysiological and Behavioral Phenotypes. *Neurotherapeutics*, **18**, 845-858.

Kutna, V., Uttl, L., Waltereit, R., Kristofikova, Z., Kaping, D., Petrasek, T., Hoschl, C. & Ovsepian, S.V. (2020) Tuberous Sclerosis (tsc2+/-) Model Eker Rats Reveals Extensive Neuronal Loss with Microglial Invasion and Vascular Remodeling Related to Brain Neoplasia. *Neurotherapeutics*, **17**, 329-339.

Lopes, D.A., Souza, T.M.O., de Andrade, J.S., Silva, M.F.S., Antunes, H.K.M., Le Sueur Maluf, L., Cespedes, I.C. & Viana, M.B. (2019) Anxiolytic and panicolytic-like effects of environmental enrichment seem to be modulated by serotonin neurons located in the dorsal subnucleus of the dorsal raphe. *Brain Res Bull*, **150**, 272-280.

Ma, T., Hoeffer, C.A., Capetillo-Zarate, E., Yu, F., Wong, H., Lin, M.T., Tampellini, D., Klann, E., Blitzer, R.D. & Gouras, G.K. (2010) Dysregulation of the mTOR pathway mediates impairment of synaptic plasticity in a mouse model of Alzheimer's disease. *PLoS One*, **5**.

Mancuso, J.J., Chen, Y., Li, X., Xue, Z. & Wong, S.T. (2013) Methods of dendritic spine detection: from Golgi to high-resolution optical imaging. *Neuroscience*, **251**, 129-140.

Marcondes, F.K., Miguel, K.J., Melo, L.L. & Spadari-Bratfisch, R.C. (2001) Estrous cycle influences the response of female rats in the elevated plus-maze test. *Physiol Behav*, **74**, 435-440.

Martin, E.I., Ressler, K.J., Binder, E. & Nemeroff, C.B. (2010) The neurobiology of anxiety disorders: brain imaging, genetics, and psychoneuroendocrinology. *Clin Lab Med*, **30**, 865-891.

Mechan, A.O., Moran, P.M., Elliott, M., Young, A.J., Joseph, M.H. & Green, R. (2002) A comparison between Dark Agouti and Sprague-Dawley rats in their behaviour on the elevated plus-maze, open-field apparatus and activity meters, and their response to diazepam. *Psychopharmacology (Berl)*, **159**, 188-195.

Meikle, L., Pollizzi, K., Egnor, A., Kramvis, I., Lane, H., Sahin, M. & Kwiatkowski, D.J. (2008) Response of a neuronal model of tuberous sclerosis to mammalian target of rapamycin (mTOR) inhibitors: effects on mTORC1 and Akt signaling lead to improved survival and function. *J Neurosci*, **28**, 5422-5432.

Miller, C.K., Halbing, A.A., Patisaul, H.B. & Meitzen, J. (2021) Interactions of the estrous cycle, novelty, and light on female and male rat open field locomotor and anxiety-related behaviors. *Physiol Behav*, **228**, 113203.

Mizuguchi, M., Takashima, S., Yamanouchi, H., Nakazato, Y., Mitani, H. & Hino, O. (2000) Novel cerebral lesions in the Eker rat model of tuberous sclerosis: cortical tuber and anaplastic ganglioglioma. *J Neuropathol Exp Neurol*, **59**, 188-196.

Ozonoff, S., Heung, K., Byrd, R., Hansen, R. & Hertz-Picciotto, I. (2008) The onset of autism: patterns of symptom emergence in the first years of life. *Autism Res*, **1**, 320-328.

Patro, N., Kumar, K. & Patro, I. (2013) Quick Golgi method: modified for high clarity and better neuronal anatomy. *Indian J Exp Biol*, **51**, 685-693.

Paxinos, G. & Watson, C. (2007) *The rat brain in stereotaxic coordinates*. Academic Press/Elsevier, Amsterdam ; Boston ;.

Peier, A.M., McIlwain, K.L., Kenneson, A., Warren, S.T., Paylor, R. & Nelson, D.L. (2000) (Over)correction of FMR1 deficiency with YAC transgenics: behavioral and physical features. *Hum Mol Genet*, **9**, 1145-1159.

Penzes, P., Buonanno, A., Passafaro, M., Sala, C. & Sweet, R.A. (2013) Developmental vulnerability of synapses and circuits associated with neuropsychiatric disorders. *J Neurochem*, **126**, 165-182.

Penzes, P., Cahill, M.E., Jones, K.A., VanLeeuwen, J.E. & Woolfrey, K.M. (2011) Dendritic spine pathology in neuropsychiatric disorders. *Nat Neurosci*, **14**, 285-293.

Petrasek, T., Vojtechova, I., Klovrza, O., Tuckova, K., Vejmola, C., Rak, J., Sulakova, A., Kaping, D., Bernhardt, N., de Vries, P.J., Otahal, J. & Waltereit, R. (2021) mTOR inhibitor improves autistic-like behaviors related to Tsc2 haploinsufficiency but not following developmental status epilepticus. *J Neurodev Disord*, **13**, 14.

Ramos, A. (2008) Animal models of anxiety: do I need multiple tests? *Trends Pharmacol Sci*, **29**, 493-498.

Reith, R.M., McKenna, J., Wu, H., Hashmi, S.S., Cho, S.H., Dash, P.K. & Gambello, M.J. (2013) Loss of Tsc2 in Purkinje cells is associated with autistic-like behavior in a mouse model of tuberous sclerosis complex. *Neurobiol Dis*, **51**, 93-103.

Rennebeck, G., Kleymenova, E.V., Anderson, R., Yeung, R.S., Artzt, K. & Walker, C.L. (1998) Loss of function of the tuberous sclerosis 2 tumor suppressor gene results in embryonic lethality characterized by disrupted neuroepithelial growth and development. *Proc Natl Acad Sci U S A*, **95**, 15629-15634.

Rochefort, N.L. & Konnerth, A. (2012) Dendritic spines: from structure to in vivo function. *EMBO Rep*, **13**, 699-708.

Schneider, M., de Vries, P.J., Schonig, K., Rossner, V. & Waltereit, R. (2017) mTOR inhibitor reverses autistic-like social deficit behaviours in adult rats with both Tsc2 haploinsufficiency and developmental status epilepticus. *Eur Arch Psychiatry Clin Neurosci*, **267**, 455-463.

Schwartzkroin, P.A., Roper, S.N. & Wenzel, H.J. (2004) Cortical dysplasia and epilepsy: animal models. *Adv Exp Med Biol*, **548**, 145-174.

Specchio, N., Pietrafusa, N., Trivisano, M., Moavero, R., De Palma, L., Ferretti, A., Vigevano, F. & Curatolo, P. (2020) Autism and Epilepsy in Patients With Tuberous Sclerosis Complex. *Front Neurol*, **11**, 639.

Stafstrom, C.E. (2005) Progress toward understanding epileptogenesis in tuberous sclerosis complex: two hits, no outs, and the Eker rat is up to bat. *Epilepsy Curr*, **5**, 136-138.

Stafstrom, C.E. (2006) Is cognition altered in the eker rat model of tuberous sclerosis complex? *Epilepsy Curr*, **6**, 210-212.

Stins, J.F. & Emck, C. (2018) Balance Performance in Autism: A Brief Overview. *Front Psychol*, **9**, 901.

Sudakov, S.K., Nazarova, G.A., Alekseeva, E.V. & Bashkatova, V.G. (2013) Estimation of the level of anxiety in rats: differences in results of open-field test, elevated plus-maze test, and Vogel's conflict test. *Bull Exp Biol Med*, **155**, 295-297.

Sztainberg, Y., Kuperman, Y., Tsoory, M., Lebow, M. & Chen, A. (2010) The anxiolytic effect of environmental enrichment is mediated via amygdalar CRF receptor type 1. *Mol Psychiatry*, **15**, 905-917.

Talkowski, M.E., Minikel, E.V. & Gusella, J.F. (2014) Autism spectrum disorder genetics: diverse genes with diverse clinical outcomes. *Harv Rev Psychiatry*, **22**, 65-75.

Tang, G., Gudsnuk, K., Kuo, S.H., Cotrina, M.L., Rosoklija, G., Sosunov, A., Sonders, M.S., Kanter, E., Castagna, C., Yamamoto, A., Yue, Z., Arancio, O., Peterson, B.S., Champagne, F., Dwork, A.J., Goldman, J. & Sulzer, D. (2014) Loss of mTOR-dependent macroautophagy causes autistic-like synaptic pruning deficits. *Neuron*, **83**, 1131-1143.

Tavazoie, S.F., Alvarez, V.A., Ridenour, D.A., Kwiatkowski, D.J. & Sabatini, B.L. (2005) Regulation of neuronal morphology and function by the tumor suppressors Tsc1 and Tsc2. *Nat Neurosci*, **8**, 1727-1734.

Tsai, P.T., Hull, C., Chu, Y., Greene-Colozzi, E., Sadowski, A.R., Leech, J.M., Steinberg, J., Crawley, J.N., Regehr, W.G. & Sahin, M. (2012) Autistic-like behaviour and cerebellar dysfunction in Purkinje cell Tsc1 mutant mice. *Nature*, **488**, 647-651.

Tsai, P.T., Rudolph, S., Guo, C., Ellegood, J., Gibson, J.M., Schaeffer, S.M., Mogavero, J., Lerch, J.P., Regehr, W. & Sahin, M. (2018) Sensitive Periods for Cerebellar-Mediated Autistic-like Behaviors. *Cell Rep*, **25**, 357-367 e354.

Tseng, C.J., McDougle, C.J., Hooker, J.M. & Zurcher, N.R. (2021) Epigenetics of Autism Spectrum Disorder: Histone Deacetylases. *Biol Psychiatry*.

Van de Weerd, H.A., Aarsen, E.L., Mulder, A., Kruitwagen, C.L., Hendriksen, C.F. & Baumans, V. (2002) Effects of environmental enrichment for mice: variation in experimental results. *J Appl Anim Welf Sci*, **5**, 87-109.

Waltereit, R., Japs, B., Schneider, M., de Vries, P.J. & Bartsch, D. (2011) Epilepsy and Tsc2 haploinsufficiency lead to autistic-like social deficit behaviors in rats. *Behav Genet*, **41**, 364-372.

Wenzel, H.J., Patel, L.S., Robbins, C.A., Emmi, A., Yeung, R.S. & Schwartzkroin, P.A. (2004) Morphology of cerebral lesions in the Eker rat model of tuberous sclerosis. *Acta Neuropathol*, **108**, 97-108.

Werling, D.M. & Geschwind, D.H. (2013) Sex differences in autism spectrum disorders. *Curr Opin Neurol*, **26**, 146-153.

Winter, S.S., Koppen, J.R., Ebert, T.B. & Wallace, D.G. (2013) Limbic system structures differentially contribute to exploratory trip organization of the rat. *Hippocampus*, **23**, 139-152.

Won, H., Mah, W. & Kim, E. (2013) Autism spectrum disorder causes, mechanisms, and treatments: focus on neuronal synapses. *Front Mol Neurosci*, **6**, 19.

Wurbel, H. (2001) Ideal homes? Housing effects on rodent brain and behaviour. *Trends Neurosci*, **24**, 207-211.

Yasuda, S., Sugiura, H., Katsurabayashi, S., Shimada, T., Tanaka, H., Takasaki, K., Iwasaki, K., Kobayashi, T., Hino, O. & Yamagata, K. (2014) Activation of Rheb, but not of mTORC1, impairs spine synapse morphogenesis in tuberous sclerosis complex. *Sci Rep*, **4**, 5155.

Yeung, R.S. (2004) Lessons from the Eker rat model: from cage to bedside. *Curr Mol Med*, **4**, 799-806.

Yeung, R.S., Katsetos, C.D. & Klein-Szanto, A. (1997) Subependymal astrocytic hamartomas in the Eker rat model of tuberous sclerosis. *Am J Pathol*, **151**, 1477-1486.

Zhou, X., Zhu, J., Liu, K.Y., Sabatini, B.L. & Wong, S.T. (2006) Mutual information-based feature selection in studying perturbation of dendritic structure caused by TSC2 inactivation. *Neuroinformatics*, **4**, 81-94.

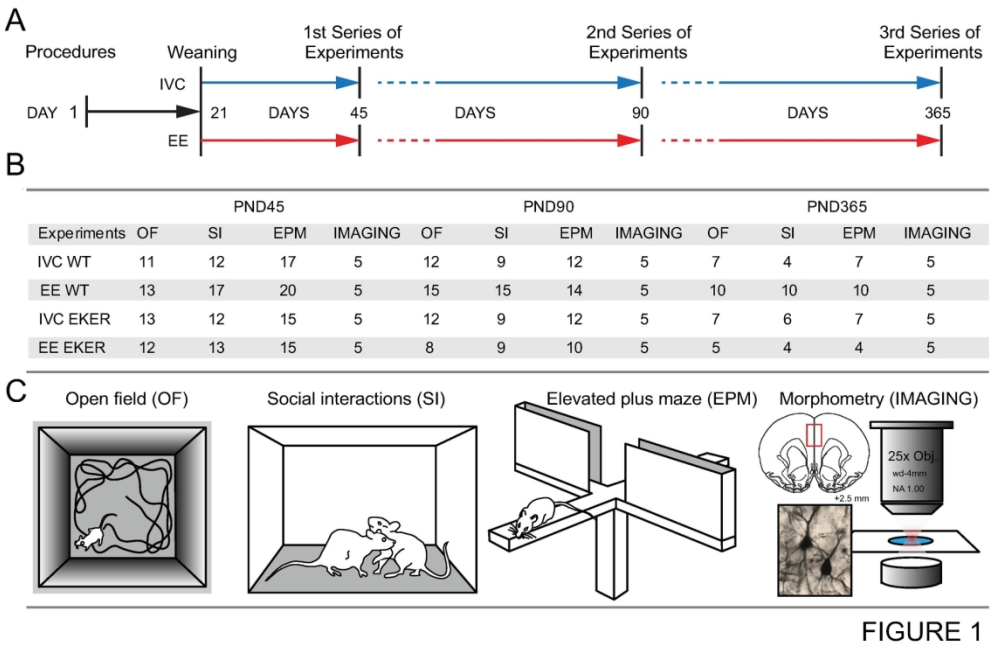

	PND45				PND90				PND365			
Experiments	OF	SI	EPM	IMAGING	OF	SI	EPM	IMAGING	OF	SI	EPM	IMAGING
IVC WT	11	12	17	5	12	9	12	5	7	4	7	5
EE WT	13	17	20	5	15	15	14	5	10	10	10	5
IVC EKER	13	12	15	5	12	9	12	5	7	6	7	5
EE EKER	12	13	15	5	8	9	10	5	5	4	4	5

Figure 1. Experiment design with illustrations of behavioural tests and morphometric analysis. (A) Experiment design. After the weaning at the postnatal day (PND) 21, rats were transferred to either an enriched environment or individually ventilated cages (EE or IVC, respectively) and subjected to behavioural tests followed by histological analysis in three age groups: PND45 (young), PND90 (adulthood) and PND365 (aged). (B) Table showing the number of rats used in various experiments of the current study. (C) Schematized representation of principal experimental paradigms utilized in this study.

159x104mm (300 x 300 DPI)

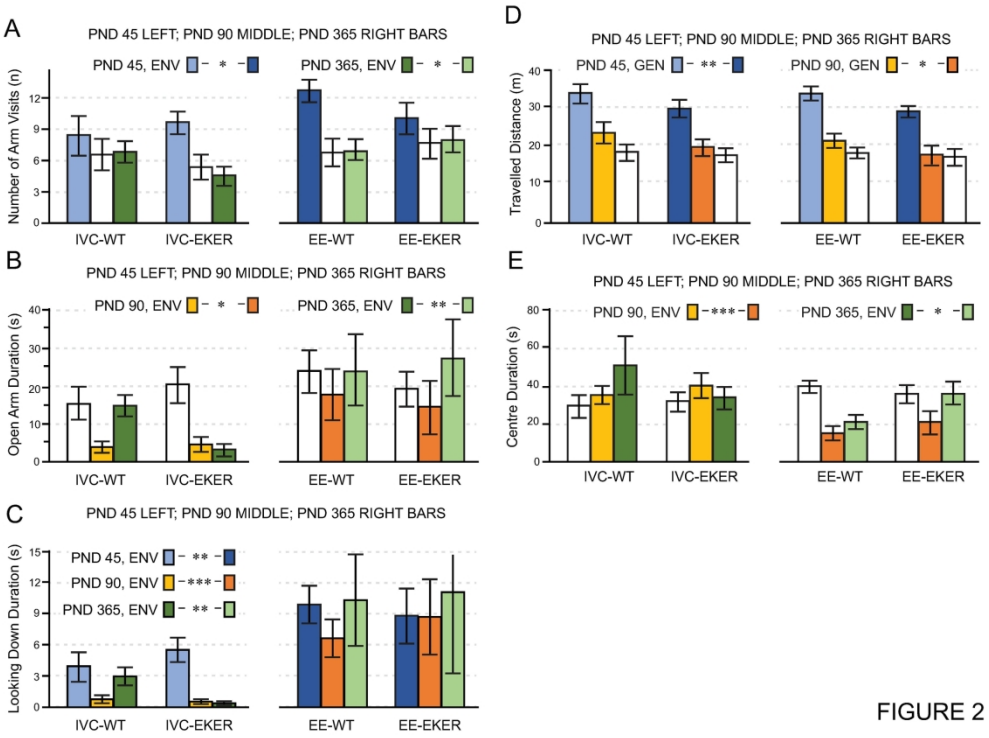

Figure 2. The impact of age, genotype, and environment on behavioural outcomes in the elevated plus-maze (A, B, C) and open field (D, E) tests. Summary bar graphs of the number of arm visits (A), time spent in the open arms (B) and duration of looking down from the maze (C). Summary bar graphs of travelled distance (D) and time spent in the centre of the open field apparatus (E). PND45 left bars; PND90 middle bars; PND365 right bars. Asterisks mark where the difference between groups reached statistical significance * $p < 0.05$, ** $p < 0.005$, *** $p < 0.0005$. White bars represent datasets with no significant difference. GEN – genotype, ENV – environment.

210x153mm (300 x 300 DPI)

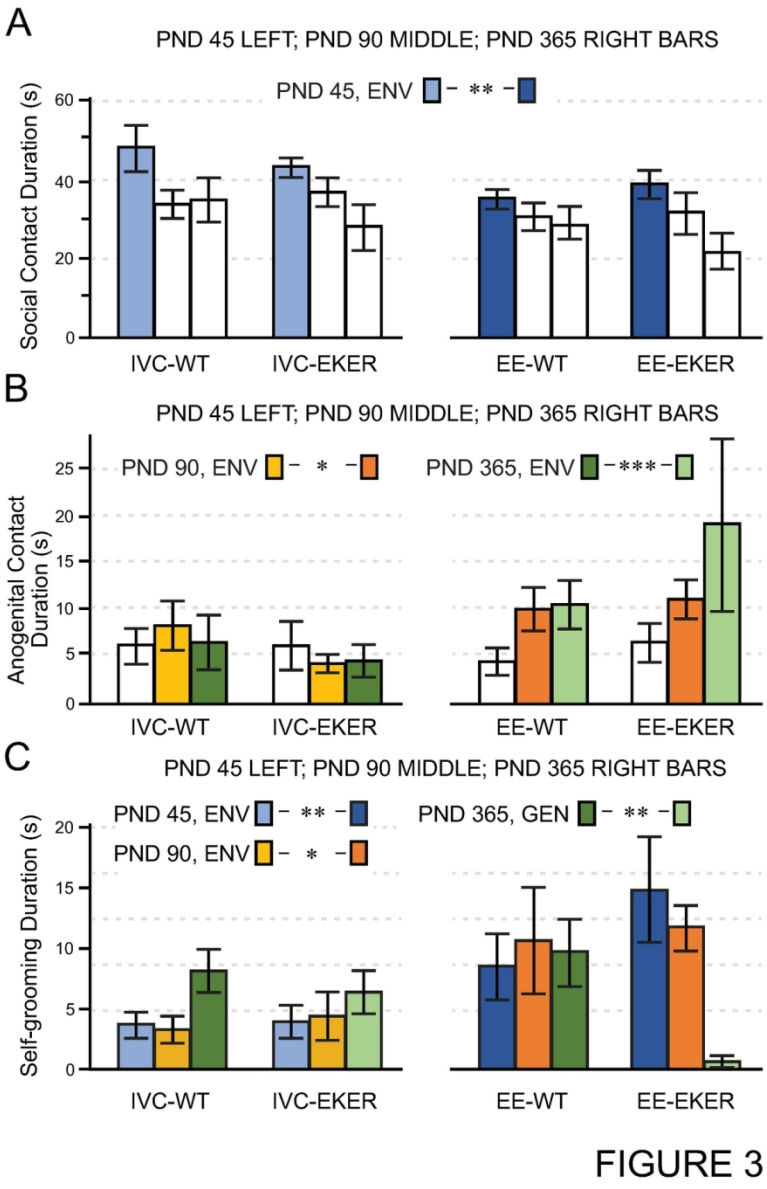

FIGURE 3

Figure 3. The impact of age, genotype, and environment on behavioural outcomes in social interaction test. Summary bar graphs of the duration of active social contact - head or body sniffing (A), anogenital exploration duration (B) and self-grooming duration (C). PND45, left bars; PND90 middle bars; PND365 right bars. Asterisks mark where the difference between groups reached statistical significance * $p < 0.05$, ** $p < 0.005$, *** $p < 0.0005$. White bars represent datasets with no significant difference. GEN – genotype. ENV – environment.

106x160mm (300 x 300 DPI)

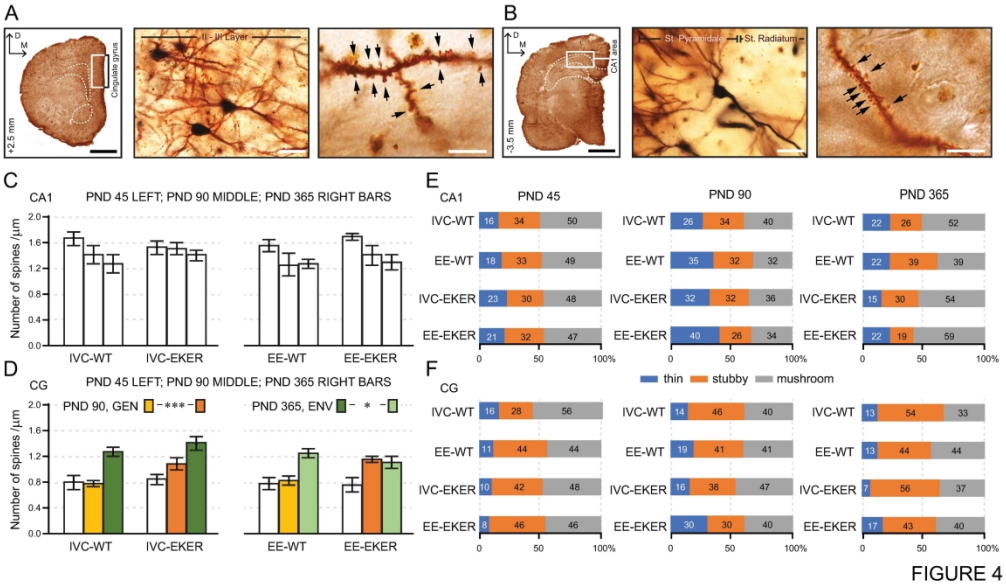

FIGURE 4

Figure 4. The impact of the age, genotype, and environment on dendritic spine density and morphology. (A, B) Representative low-magnification images of Golgi rapid stained slices: the cingulate gyrus, bregma +2.5 mm; dorsal hippocampus, bregma -3.5. Rectangles mark the anatomical locations where dendritic spines were analysed. D – dorsal, M – medial. Scale bars: 1.0 mm. (A) Representative light microscopic images of pyramidal neurons with apical and basal dendrites in layer II-III of the cingulate gyrus (middle and right) and (B) CA1 region of the hippocampus (middle and right). Scale bars 15 µm. High-magnification images of secondary dendritic branches with dendritic spines from the prefrontal cortex and hippocampus (A, B: right panels). Black arrows point at individual spines. Scale bars 5 µm. Summary bar graphs of the mean spine density in the CA1 region of the hippocampus (C) and cingulate gyrus (CG) (D). Postnatal days: PND45, left bars; PND90 middle bars; PND365 right bars. Asterisks mark statistically significant differences indicated by two-way ANOVA, with a degree of significance * $p < 0.05$, ** $p < 0.005$. White bars represent datasets with no difference. (E, F) Summary stacked bars representing the fraction (number insets) of three main morphological variants of dendritic spines: thin spines, marked in blue; stubby spines in orange, and mushroom spines in grey. The graphs present data from five rats of each experimental group for individual data points (n = 5). GEN – genotype, ENV – environment.

247x144mm (300 x 300 DPI)

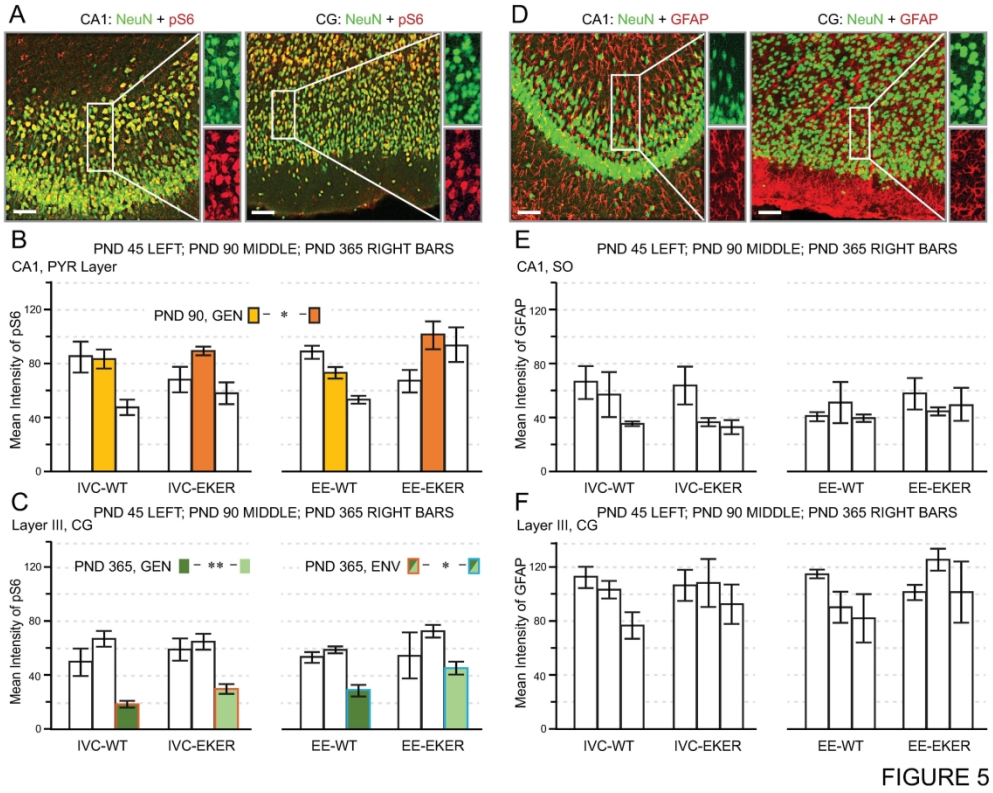

Figure 5. The impact of age, genotype, and environment on neuronal and astrocyte markers NeuN and GFAP and mTOR activation marker pS6. (A, D) Representative immunofluorescence images of hippocampal CA1 (left panels) and cingulate gyrus (CG) areas (right panels) in coronal brain slices stained for the neuronal marker NeuN (green), a marker of mTOR activation pS6 (red; A), and an astrocyte marker GFAP (red; D). Narrow right insets show an enlarged view of stratum oriens (SO) of the CA1 region of the hippocampus (left panels) and layer III of the CG (right panels). CA1 scale bars 75 μm. Cingulate gyrus scale bars 100 μm. (B, C) Summary bar graphs of the mean intensity of pS6 signal in the stratum pyramidale (PYR Layer) of the CA1 region (B) and layer III of the cingulate gyrus (C). (E, F) Summary graphs of the mean intensity of GFAP in the stratum oriens of the CA1 region (E) and layer 3 of the CG (F). Asterisks mark the results of comparison reaching statistical significance, using two-way ANOVA, with a degree of significance * $p < 0.05$, ** $p < 0.005$. White bars represent datasets with no significant difference. Postnatal day (PND) 45, left bars; PND90 middle bars; PND365 right bars. The graphs present data from three rats of each experimental group for each data point (n = 3), with intensity measurements pulled from 9 regions of interest (ROIs) quantified per animal. GEN – genotype, ENV – environment.

209x166mm (300 x 300 DPI)

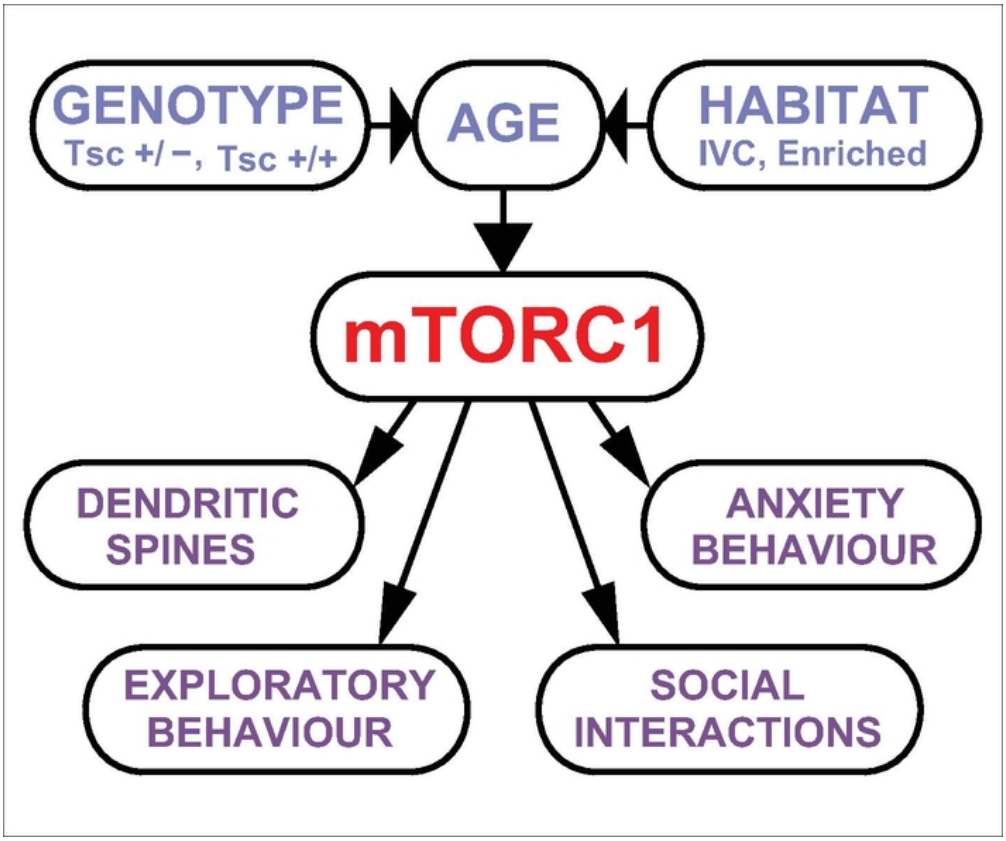

Graphical abstract
Schematic representation of the key factors shaping the histopathological profile with affected neurobehavioral domains in autism spectrum disorder (ASD) Eker rat. The effects of age, genotype and environment converge on mTORC1 signalling pathway leading to alterations in neuronal plasticity with behavioural impairments.

60x50mm (300 x 300 DPI)